Relaxed Astrophysical Solutions in Non-Minimally Coupled Models

Aníbal José Ferreira e Silva
Mestrado em Física
Departamento de Física e Astronomia
2017

Orientador
Jorge Tiago Almeida Páramos, Professor auxiliar convidado, Faculdade de Ciências da Universidade do Porto

U.PORTO

FACULDADE DE CIÊNCIAS
UNIVERSIDADE DO PORTO

Todas as correções determinadas pelo júri, e só essas, foram efetuadas.

O Presidente do Júri,

Porto, _____/_____/_____

“ Imagination will often carry us to worlds that never were. But without it we go nowhere. ”

Carl Sagan

Acknowledgements

First of all, I would like to give a special thank you to my family, not only for providing constant support along these years, but also for encouraging me to never give up my academic life.

Secondly, I would like to thank my supervisor, Professor Jorge Páramos, for accepting me as his student and for all the help and discussions over the last year: it was a great pleasure to work with you.

Finally, I would like to give a word of appreciation to all my friends. In particular, a word of affection to Maria, for always believing in me and for being there for me when I most needed.

UNIVERSIDADE DO PORTO

Abstract

Faculdade de Ciências da Universidade do Porto
Departamento de Física e Astronomia

Master of Science

Relaxed Astrophysical Solutions in Non-Minimally Coupled Models

by Aníbal José Ferreira e
Silva

In this thesis we study a class of modified theory of gravity known as Non-Minimally Coupled (NMC) models from an astrophysical point of view. We focus this study on one of the most challenging subjects in physics at the present time — Dark Matter. Using NMC theories, which consist in a phenomenological extension of the action functional involving arbitrary functions of the scalar curvature, one of which is coupled with matter, we show that it is possible to mimic the behavior of dark matter in the outer regions of galaxies which exhibit spherical symmetry, under a regime which we dub as "relaxed". Analytical solutions to our physically relevant quantities are presented, and later compared with the standard dark matter and visible density profiles. Finally, we link our results with observations, hence obtaining constrains on the model parameters. This thesis is based in the work developed in Ref. [1].

UNIVERSIDADE DO PORTO

Resumo

Faculdade de Ciências da Universidade do Porto
Departamento de Física e Astronomia

Mestre de Ciência

Soluções Astrofísicas Relaxadas em Modelos com Acoplamento Não-Mínimo

por Aníbal José Ferreira e Silva

Nesta tese estudamos uma classe de teorias alternativas da gravidade, conhecidas como modelo com acoplamento não-mínimo, num contexto astrofísico. Com esta teoria, focamos o nosso estudo num dos mais desafiantes problemas da física no presente — a matéria escura.

Usando esta teoria alternativa, que consiste numa forma fenomenológica de extender o funcional da acção através de funções arbitrárias do escalar de curvatura, uma das quais se encontra acoplada com a matéria, mostramos que é possível imitar o comportamento da matéria escura nas partes exteriores de galáxias com simetria esférica, num regime que identificamos como "relaxado". Com isto, apresentamos soluções analíticas para as quantidades físicas de interesse, comparando-as depois com as distribuições usuais de densidade encontradas na literatura. Finalmente, ligamos os nossos resultados com dados observacionais, de modo a obter restrições para os parâmetros do modelo.

Esta tese é baseada no trabalho desenvolvido na Ref. [1].

Contents

Acknowledgements iii

Abstract v

Resumo vii

Contents ix

List of Figures xi

List of Tables xiii

Abbreviations xv

1 Introduction 1

2 General Relativity and Alternative Theories of Gravity 5
- 2.1 Einstein-Hilbert Action . . . 5
- 2.2 Birkhoff Metric . . . 6
- 2.3 Interior Solutions . . . 7
- 2.4 Conformal Transformations . . . 9
  - 2.4.1 Energy-Momentum Tensor . . . 10
- 2.5 Equivalence Between GR and a Scalar Field Theory . . . 12
- 2.6 $f(R)$ Action . . . 14
  - 2.6.1 Equivalence Between $f(R)$ and Scalar Field Theory . . . 15

3 Non-Minimal Coupling Model 17
- 3.1 Field Equations . . . 17
- 3.2 Non-Conservation of Energy-Momentum Tensor . . . 18
- 3.3 Choice of the Lagrangian . . . 19
- 3.4 Equivalence Between NMC and Scalar Field Theory . . . 21

4 Relaxed Non-Minimally Coupled Regime 23
- 4.1 Dark Matter Mimicking . . . 24

4.2 Stationary Case . . . 25
4.3 Analytical Solution . . . 27

5 Matter Profiles and Constrains to the Model 33
5.1 Standard Matter Profiles . . . 33
5.1.1 Cusped Profiles . . . 34
5.1.2 Hernquist Visible Matter Profile . . . 34
5.1.3 Navarro-Frenk-White Dark Matter Profile . . . 35
5.1.4 Isothermal Dark Matter Profile . . . 35
5.2 Mass Budget . . . 37
5.2.1 Mass . . . 37
5.3 Energy Conditions . . . 38
5.4 Model Parameter Constraints . . . 39

6 Conclusions 43

List of Figures

5.1 Low curvature regime 41

List of Tables

5.1 Outer region behavior for the relevant profiles 36
5.2 Data obtained by performing a fit to rotational curves of galaxies. . . . 40

Abbreviations

GR	**G**eneral **R**elativity
NMC	**N**on-**M**inimal **C**oupling
EOS	**E**quation **O**f **S**tate
NFW	**N**avarro-**F**renk-**W**hite
DM	**D**ark **M**atter
TOV	**T**olman-**O**ppenheimer-**V**olkoff
JBD	**J**ordan-**B**rans-**D**icke

Chapter 1

Introduction

It has been roughly a century since Albert Einstein formulated the theory of General Relativity (GR). Since then, his insightful and elegant perception of gravity and space-time gave us new ways of understanding our universe, from the local to the cosmological scale, (see *e.g.* Refs. [2, 3]). Indeed, very recently, the existence of gravitational waves was confirmed through the observation of a merger of two black holes [4].

Notwithstanding, GR does not fully account for the current observations of the Universe. For instance, it fails to explain the large scale accelerated expansion of the Cosmos, without the need to invoke some exotic content of matter such as dark energy [5]. Even with this *a priori* approach, a satisfactory justification regarding the gap between the measured and theoretically obtained vacuum energy is still to be found [6].

Another fundamental aspect which GR cannot adequately explain is galactic structure formation. The inconsistency between rotational curves in the outer regions of a galaxy, where the rotational velocity flattens, tells us that there should be an extra contribution to the total mass of a given galaxy. This also calls for the need of another type of matter, the so called dark matter [7].

Dark matter has been catalogued as one of the most exciting problems in physics: a "mysterious mist" that envelops galaxies and galaxy clusters and keeps them gravitationally bound, thus providing local structure to our universe. Its gravitational pull is so strong that it bends light passing trough it, mimicking the effect of a lens. This effect does not only provide us with an insight on how much dark matter our universe is composed of, but also reveals its spatial distribution. One of the most important discoveries so far is the so called Bullet cluster [8], where direct evidence of dark matter was observed by a merger between two galaxy clusters.

According to Newton's law of gravity, the rotation curve of a given galaxy with spherical symmetry follows the equation

$$v^2(r) = \frac{GM(r)}{r} \quad , \tag{1.1}$$

so we should expect a velocity decrease in the outer regions, $v \sim r^{-1/2}$. Instead, observations show that the rotation curve is approximately flat, $v \sim const.$: to compensate the radial increase, we can posit that there must be an extra contribution to the total mass of a given galaxy.

A more radical way of thinking comes from modified Newtonian dynamics (MOND). This proposal, first introduced by Milgrom [9] (see Ref. [10] for a discussion), consists in a modification of Newton's second law, by the introduction of a acceleration parameter a_0

$$\mathbf{F} = m_g \mu \left(\frac{a}{a_0} \right) \mathbf{a} \quad , \tag{1.2}$$

where μ is an interpolating function such that

$$\mu \sim \begin{cases} 1, & a \gg a_0 \quad , \\ \frac{a}{a_0}, & a \ll a_0 \quad , \end{cases} \tag{1.3}$$

so at large distances, Newton's gravitational law implies

$$\frac{a^2}{a_0} = \frac{GM}{r^2} \quad , \tag{1.4}$$

which yields a constant rotational velocity

$$v^4 = GMa_0 \quad , \tag{1.5}$$

with $a_0 \sim 2 \times 10^{-10}$ m/s^2. This proposal provides good agreements with rotation curves, without the need to invoke "exotic" dark matter components [11]. However, this theory relies in some axioms which still need to be proven experimentally, and has a rather awkward relativistic formulation [12].

Another approach to solve this problem relies on a phenomenological modification of the Einstein-Hilbert action functional: the class of $f(R)$ theories, which essentially consists in replacing the linear scalar curvature term by an arbitrary function of it [13]. This model can, for instance, describe the mechanism behind inflation, by adding a quadratic term to the Lagrangian density, which dominates at early times [14].

More generally, one can also insert a non-minimal coupling (NMC) between an arbitrary function of the scalar curvature and the Lagrangian density of matter [15, 16];

this can arise from one-loop vacuum-polarization effects in the formulation of Quantum Electrodynamics in a curved space-time [17] or from considering a Riemann-Cartan geometry [18]. In recent years, this theory has been carefully studied and has yielded several interesting results [19–27], while avoiding potential pitfalls [28, 29] (see Ref. [30] for a discussion).

Taking these considerations into account, in this thesis we aim to expand upon the mechanism to mimic dark matter in the outer regions of galaxies resorting to a NMC model in a relaxed regime, as first described in Ref. [31]. For simplicity, we restrict the analysis to galaxies which exhibit spherical symmetry, composed of a perfect fluid.

The layout of this thesis is as follows: In Chapter 2, we give a motivation to the use of NMC theories. In Chapter 3 we introduce the model under study and present some of its properties. In Chapter 4, we delve in our calculations, starting by what we call the "relaxed regime", aiming to show that is possible to obtain an appropriate dark matter mimicked profile for the model under scrutiny. In Chapter 5, we compare our solutions with the standard models in the literature and constrain our parameters. Finally, overall conclusions are presented in Chapter 6.

Chapter 2

General Relativity and Alternative Theories of Gravity

In this chapter we start by introducing the Einstein-Hilbert action and then proceed to derive the interior solution that describes the spacetime and energy structure of a given object. Also, an introduction to conformal transformations will be given. Next, we show how a conformal transformation induces an equivalence between GR and the Jordan-Brans-Dicke theory. Later, we provide some introductory remarks about phenomenological $f(R)$ theories.

2.1 Einstein-Hilbert Action

Although Einstein's theory of gravity was primarily constructed from the mathematical description of differential manifolds, where the spacetime structure is non-Euclidean, it can also be described through a Lagrangian formalism. Hilbert proposed the simplest Lagrangian, so that the correspondent action functional reads

$$S_{EH} = \int d^4x\sqrt{-g}\,(\kappa R + \mathcal{L}_m) \quad , \tag{2.1}$$

where g denotes the determinant of the metric, $\kappa = c^4/16\pi G$, where G is the gravitational constant and c denotes the speed of light in vacuum and $\mathcal{L}_m$ is the Lagrangian density of matter. From now on, we will take $c = 1$ unless stated otherwise.

Variation of the action functional with respect to the metric yields the Einstein field equations

$$G_{\mu\nu} = \frac{8\pi G}{c^4} T_{\mu\nu} \quad , \tag{2.2}$$

where $G_{\mu\nu}$ is the Einstein tensor defined as

$$G_{\mu\nu} = R_{\mu\nu} - \frac{1}{2} g_{\mu\nu} R \quad , \tag{2.3}$$

while $T_{\mu\nu}$ is the energy-momentum tensor defined as

$$T_{\mu\nu} = -\frac{2}{\sqrt{-g}} \frac{\delta(\sqrt{-g}\mathcal{L}_m)}{\delta g^{\mu\nu}} \quad . \tag{2.4}$$

2.2 Birkhoff Metric

One of the outstanding results concerning the structure of spacetime in General Relativity comes from the Birkhoff Theorem: it states that any spherically symmetric solution of the vacuum field equations possesses a timelike Killing vector. The mathematical structure behind this theorem is composed by four Killing vector fields ξ_μ *i.e.*, vectors that satisfy the Killing equation:

$$\nabla_\mu \xi_\nu = -\nabla_\nu \xi_\mu \quad , \tag{2.5}$$

where ∇_μ is the covariant derivative. Three of these vectors are spacelike and, for a spherical symmetric object, they are isomorphic to the generators of $SO(3)$, the rotation group, and satisfy the closed Lie algebra

$$[L_i, L_j] = \epsilon_{ijk} L_j \quad , \tag{2.6}$$

where ϵ_{ijk} is the Levi-Civita tensor. They are defined as

$$L_1 = \partial_\phi \quad , \tag{2.7}$$

$$L_2 = \cos\phi \, \partial_\theta - \cot\theta \sin\phi \, \partial_\phi \quad , \tag{2.8}$$

$$L_3 = -\sin\phi \, \partial_\theta - \cot\theta \cos\phi \, \partial_\phi \quad . \tag{2.9}$$

The line element under these generators is written as

$$d\Sigma^2 = d\theta^2 + \sin^2\theta d\phi^2 \quad , \tag{2.10}$$

which produces the unit sphere S^2.

In a four-dimensional spacetime, we can write the line element as

$$ds^2 = -e^{2\phi(r,t)} dt^2 + e^{2\lambda(r,t)} dr^2 + r^2 d\Sigma^2 \quad , \tag{2.11}$$

where $\phi(r,t)$ and $\lambda(r,t)$ are arbitrary functions. The last Killing vector is obtained by solving the Einstein field equations in vacuum, *i.e.* by setting $T_{\mu\nu} = 0$ in Eq. (2.2). The relevant components are given by

$$R_{tr} = \frac{2}{r}\partial_t \lambda = 0 \quad , \tag{2.12}$$

which sets $\lambda(t,r) = \lambda(r)$. The other one is

$$R_{\theta\theta} = e^{-2\lambda}\left[r(\partial_r\lambda - \partial_r\phi) - 1\right] + 1 = 0 \quad . \tag{2.13}$$

Differentiating with respect to time, this yields

$$\partial_t\partial_r\phi = 0 \rightarrow \phi(r,t) = f(r) + g(t) \quad . \tag{2.14}$$

So that $g_{tt} = -e^{2f(r)}e^{2g(t)}$. Noting that we can always redefine our time coordinate as $dt \rightarrow e^{-g(t)}dt$ and, setting $g(t) = 0$, we finally obtain the eponymous Birkhoff metric:

$$ds^2 = -e^{2\phi(r)}dt^2 + e^{2\lambda(r)}dr^2 + r^2 d\Sigma^2 \quad , \tag{2.15}$$

we see that our metric elements are time independent, which implies that the last Killing vector field is timelike.

2.3 Interior Solutions

One of the most interesting and fundamental results regarding GR lies in the solutions which describe the interior of a spherical symmetric object, like a star.

We consider that our object is described by a perfect and isotropic fluid

$$T_{\mu\nu} = (p + \rho)u_\mu u_\nu + p g_{\mu\nu} \quad , \tag{2.16}$$

where $\rho = \rho(r)$ denotes the energy density, $p = p(r)$ the pressure, and u_μ the 4-velocity vector field, with components $u_\mu = (u_0, 0, 0, 0)$ (assuming the fluid at rest), normalized $u_\mu u^\mu = -1$ and with a vanishing gradient field: $u_\mu \nabla_\nu u^\mu = 0$. Notice that, since the energy-momentum tensor is diagonal and time independent, the Birkhoff metric (2.15) can be adopted to this model.

Taking the trace of the Einstein field equation (2.2) we find that

$$R = -8\pi G T \quad , \tag{2.17}$$

so that Eq. (2.2) can be written as:

$$R_{\mu\nu} = 8\pi G\left(T_{\mu\nu} - \frac{1}{2}g_{\mu\nu}T\right) \quad . \tag{2.18}$$

The non-vanishing and independent components of this equation are

$$e^{-2\lambda}\left(\phi'' + (\phi')^2 - \phi'\lambda' + \frac{2\phi'}{r}\right) = 4\pi G(3p+\rho) \quad , \tag{2.19}$$

$$-e^{-2\lambda}\left(\phi'' + (\phi')^2 - \phi'\lambda' - \frac{2\lambda'}{r}\right) = 4\pi G(\rho - p) \quad , \tag{2.20}$$

$$e^{-2\lambda}\left(\frac{\lambda' - \phi'}{r}\right) + \frac{1-e^{-2\lambda}}{r^2} = 4\pi G(\rho - p) \quad . \tag{2.21}$$

Adding (2.19) and (2.20) yields

$$e^{-2\lambda}\left(\frac{\phi' + \lambda'}{r}\right) = 4\pi G(\rho + p) \quad . \tag{2.22}$$

Now, adding (2.22) and (2.21) in order to eliminate ϕ' and p, one has

$$e^{-2\lambda}\left(\frac{2\lambda'}{r} - \frac{1}{r^2}\right) + \frac{1}{r^2} = 8\pi G\rho \quad . \tag{2.23}$$

Given the background knowledge of the Schwarzchild solution, we re-define our metric component g^{rr} as

$$e^{-2\lambda(r)} = 1 - \frac{2Gm(r)}{r} \quad . \tag{2.24}$$

Physically, this can be seen as a straightforward extension of the Schwarzchild metric to the interior of an object. Noticing that

$$e^{-2\lambda}\left(\frac{2\lambda'}{r} - \frac{1}{r^2}\right) + \frac{1}{r^2} = \frac{2Gm'}{r^2} \quad , \tag{2.25}$$

Eq. (2.23) becomes

$$m' = 4\pi\rho r^2 \quad , \tag{2.26}$$

which, upon integration, yields

$$m(r) = 4\pi\int \rho(r')r'^2 dr' \quad . \tag{2.27}$$

Thus confirming that $m(r)$ gives the enclosed mass within a sphere of radius r. Subtracting (2.22) with (2.21) in order to eliminate λ' and ρ, yields after some algebra, the relation

$$\phi' = G\frac{4\pi pr^3 + m}{r(r-2Gm)} \quad , \tag{2.28}$$

which, upon integration, defines the element g_{tt} as

$$e^{2\phi(r)} = \exp\left(2G\int \frac{4\pi p(r')r'^3 + m(r')}{r'\left(r' - 2Gm(r')\right)}dr'\right) \quad . \tag{2.29}$$

Thus, we can entirely define the spacetime geometry in terms of physical variables. Obviously, pressure and energy density profile are still to be known. However, there is still one last equation which can reduce our problem to a single degree of freedom. This equation can be found in the conservation of the energy momentum tensor. Taking the covariant derivative of the Einstein field equation (2.2) and resorting to the Bianchi identity $\nabla_\mu G^{\mu\nu} = 0$, one has

$$\nabla_\mu T^{\mu\nu} = 0 \quad , \tag{2.30}$$

taking the only non trivial component, $\nu = r$, yields

$$\phi' = -\frac{p'}{\rho + p} \quad , \tag{2.31}$$

which essentially sets a drag force due to the pressure gradient of the fluid. Replacing this in (2.28), one thus arrives at the Tolman-Oppenheimer-Volkoff (TOV) equation, the relativistic version of the hydrostatic equilibrium equation:

$$p' = -(\rho + p)\frac{4\pi G p r^3 + Gm}{r(r - 2Gm)} \quad . \tag{2.32}$$

Since Eqs. (2.27) and (2.32) form a system of two equations for three variables, to solve this explicitly we need to give some *a priori* information for the system under scrutiny: this can be supplied by an equation of state (EOS), $p = p(\rho)$ that specifies the intrinsic behavior of the assumed matter type.

2.4 Conformal Transformations

Given the metric $g_{\mu\nu}$, a conformal transformation is defined as

$$\tilde{g}_{\mu\nu}(x) = \Omega^2(x) g_{\mu\nu}(x) \quad , \tag{2.33}$$

with an inverse

$$\tilde{g}^{\mu\nu}(x) = \Omega^{-2}(x) g^{\mu\nu}(x) \quad , \tag{2.34}$$

where $\Omega(x)$ is the conformal factor. In here, we will concern our attention to the simple case where Ω is a global conformal factor, *i.e.*, a constant, which implies a scaling transformation of the metric. Below, we will show that in order to have an

invariantly conformed theory of gravity a scalar field must be introduced, remarkably yielding a Brans-Dicke theory of gravity. Setting $\Omega(x) \equiv \Omega$, a global conformal factor simply implies a scaling property of the metric.

Considering the infinitesimal line element:

$$ds^2 = g_{\mu\nu}(x)dx^\mu dx^\nu \quad , \tag{2.35}$$

it is easy to see that it is transformed accordingly to:

$$d\tilde{s}^2 = \Omega^2 ds^2 \quad . \tag{2.36}$$

It is important to remark that this transformation only affects spacetime structure, *i.e.,* the coordinates x^μ remain fixed. Also, they preserve the angle between two geodesics.

With the metric, we can calculate how the relevant quantities transform accordingly. For the connection, we have

$$\tilde{\Gamma}^\alpha_{\ \mu\nu} = \Gamma^\alpha_{\ \mu\nu} \quad , \tag{2.37}$$

since $\Gamma \sim g^{-1}\partial g$. This implies that the Riemann tensor also remains invariant under this transformations

$$\tilde{R}^\mu_{\ \nu\alpha\beta} = R^\mu_{\ \nu\alpha\beta} \quad , \tag{2.38}$$

and so does the Ricci scalar

$$\tilde{R}_{\mu\nu} = R_{\mu\nu} \quad . \tag{2.39}$$

However, the Ricci scalar gets a multiplicative factor

$$\tilde{R} = \tilde{g}^{\mu\nu}\tilde{R}_{\mu\nu} = \Omega^{-2}g^{\mu\nu}R_{\mu\nu} = \Omega^{-2}R \quad . \tag{2.40}$$

Finally, the d' Alembertian $\Box$, is transformed accordingly to

$$\tilde{\Box} = \tilde{g}^{\mu\nu}\nabla_\mu\nabla_\nu = \Omega^{-2}g^{\mu\nu}\nabla_\mu\nabla_\nu = \Omega^{-2}\Box \quad . \tag{2.41}$$

2.4.1 Energy-Momentum Tensor

Given the prescription above, it is interesting to see how the relevant physical quantities transform. We start by writing the physical part of the action functional S, which should be naturally invariant under these transformations, since it should not depend on how we stretch or contract our manifold. We have that:

$$S = \int d^4x\sqrt{-g}\mathcal{L} \quad . \tag{2.42}$$

Noticing that, in 4-dimensions, $\sqrt{-\tilde{g}} = \Omega^4\sqrt{-g}$ and imposing the invariance of the action functional, one has

$$\tilde{S} = S \to \int d^4x\sqrt{-\tilde{g}}\tilde{\mathcal{L}} = \int d^4x\sqrt{-g}(\Omega^4\tilde{\mathcal{L}}) \equiv \int d^4x\sqrt{-g}\mathcal{L} \quad , \tag{2.43}$$

so the invariance of the action functional is ascertained if the Lagrangian density is transformed as

$$\tilde{\mathcal{L}} = \Omega^{-4}\mathcal{L} \quad . \tag{2.44}$$

Given this, the energy-momentum tensor is conformally transformed as

$$\tilde{T}_{\mu\nu} = -\frac{2}{\sqrt{\tilde{g}}}\frac{\delta}{\delta\tilde{g}^{\mu\nu}}\left(\sqrt{-\tilde{g}}\tilde{\mathcal{L}}\right) = -\Omega^{-2}\frac{2}{\sqrt{-g}}\frac{\delta}{\delta g^{\mu\nu}}\left(\sqrt{-g}\mathcal{L}\right) = \Omega^{-2}T_{\mu\nu} \quad . \tag{2.45}$$

As an standard example, let us consider the energy-momentum tensor of a perfect and isotropic fluid:

$$T_{\mu\nu} = (\rho + p)u_\mu u_\nu + pg_{\mu\nu} \quad . \tag{2.46}$$

Considering that our fluid moves along a geodesic, so that

$$u_\mu = \frac{dx_\mu}{ds} = g_{\mu\alpha}\frac{dx^\alpha}{ds} \quad , \tag{2.47}$$

in the conformal frame, one has

$$\tilde{u}_\mu = \tilde{g}_{\mu\alpha}\frac{dx^\alpha}{d\tilde{s}} = \Omega g_{\mu\alpha}\frac{dx^a}{ds} = \Omega u_\mu \quad . \tag{2.48}$$

Thus, we get

$$\tilde{T}_{\mu\nu} = (\tilde{\rho} + \tilde{p})\,\tilde{u}_\mu\tilde{u}_\nu + \tilde{p}\tilde{g}_{\mu\nu} = \Omega^2\left[(\tilde{\rho} + \tilde{p})\,u_\mu u_\nu + \tilde{p}g_{\mu\nu}\right] \quad , \tag{2.49}$$

using Eq. (2.45), we have that

$$\Omega^{-2}\left[(\rho + p)u_\mu u_\nu + pg_{\mu\nu}\right] = \Omega^2\left[(\tilde{\rho} + \tilde{p})\,u_\mu u_\nu + \tilde{p}g_{\mu\nu}\right] \quad , \tag{2.50}$$

and this is trivially satisfied if

$$\tilde{\rho} = \Omega^{-4}\rho \ , \tag{2.51}$$

$$\tilde{p} = \Omega^{-4}p \ . \tag{2.52}$$

2.5 Equivalence Between GR and a Scalar Field Theory

In Section 2.4, we saw how the relevant tensors and scalars of GR transform by performing a conformal transformation of the metric. However, that was the simplest case where the scaling parameter Ω simply implies a global rescaling of the metric. A more general approach comes from taking a local conformal factor $\Omega = \Omega(x)$. For that purpose, we start by writing the D dimensional action functional in the so called Einstein frame in vacuum as (see Ref. [32])

$$\tilde{S} = \frac{\epsilon}{2}\int d^D x\sqrt{-\tilde{g}}\tilde{R} \ , \tag{2.53}$$

where

$$\epsilon = \frac{1}{4}\frac{D-2}{D-1} \ , \tag{2.54}$$

where, in 4-dimensions, has units $[\mathrm{M}^2]$. For a local conformal factor, the Ricci scalar and the metric determinant are transformed accordingly to

$$\tilde{R} = \Omega^{-2}\left(R - 2(D-1)\frac{\Box\Omega}{\Omega} - (D-1)(D-4)g^{\mu\nu}\frac{\Omega_{,\mu}\Omega_{,\nu}}{\Omega^2}\right) \ , \tag{2.55}$$

and

$$\sqrt{-\tilde{g}} = \Omega^D\sqrt{-g} \ , \tag{2.56}$$

so that the action functional becomes

$$S = \frac{\epsilon}{2}\int d^4 x\sqrt{-g}\Omega^{D-2}\left(R - 2(D-1)\frac{\Box\Omega}{\Omega} - (D-1)(D-4)g^{\mu\nu}\frac{\Omega_{,\mu}\Omega_{,\nu}}{\Omega^2}\right) \ , \tag{2.57}$$

which is clearly not conformally invariant, unless we take the particular case where $\Omega = constant$ and $D = 2$.

In order to obtain a conformal invariant theory, we introduce a scalar field that modifies the action functional (2.53) according to

$$\tilde{S} = \frac{\epsilon}{2}\int d^D x\sqrt{-\tilde{g}}\tilde{R}\tilde{\Phi}^2 \ . \tag{2.58}$$

This is the so called Jordan frame, where the scalar curvature is not decoupled from other matter fields. Inserting once again our conformally transformed variables, with the redefined scalar field

$$\tilde{\Phi} = \Omega^{\frac{2-D}{2}}\Phi \quad , \tag{2.59}$$

leads to the action functional

$$\tilde{S} = \frac{1}{2}\int d^D x\sqrt{-g}\Phi^2\left[\epsilon R - \frac{D-2}{2}\frac{\Box\Omega}{\Omega} - \frac{1}{4}(D-2)(D-4)g^{\mu\nu}\frac{\Omega_{,\mu}\Omega_{,\nu}}{\Omega^2}\right] \quad . \tag{2.60}$$

Adding the dynamical term

$$S_{\tilde{\Phi}} = -\frac{1}{2}\int d^D x\sqrt{-\tilde{g}}\tilde{\Phi}\tilde{\Box}\tilde{\Phi} \quad , \tag{2.61}$$

leads to

$$\tilde{S} = \frac{1}{2}\int d^D x\sqrt{-\tilde{g}}\tilde{\Phi}\left(\epsilon\tilde{R}\tilde{\Phi} - \tilde{\Box}\tilde{\Phi}\right) \quad , \tag{2.62}$$

which is in fact conformal invariant since

$$S = \frac{1}{2}\int d^D x\sqrt{-g}\Phi\left(\epsilon R\Phi - \Box\Phi\right) \quad , \tag{2.63}$$

under the correspondingly transformation law for the d'Alembertian operator. From this we conclude that, in order to obtain a conformal invariant theory of gravity, one must add a scalar field to the action functional with a specific coupling to curvature.

Another important aspect that arises from this formalism is the equivalence with the Jordan-Brans-Dicke (JBD) theory of gravity [33]. To see this clearly, we note that, for a scalar, the d'Alembertian can be written as

$$\Box\Phi = \frac{1}{\sqrt{-g}}\partial_\mu\left(\sqrt{-g}\partial^\mu\Phi\right) \quad , \tag{2.64}$$

so that

$$S = \frac{1}{2}\int d^D x\sqrt{-g}\Phi\left(\epsilon R\Phi - \frac{1}{\sqrt{-g}}\partial_\mu\left(\sqrt{-g}\partial^\mu\Phi\right)\right) \quad , \tag{2.65}$$

integrating the second term by parts, fixing the boundary at the infinity and using Stoke's theorem so that the boundary contribution leads to a zero result, yields

$$S = \frac{1}{2}\int d^D x\sqrt{-g}\left[\epsilon R\Phi^2 + \partial_\mu\Phi\partial^\mu\Phi\right] \quad , \tag{2.66}$$

which strikingly resembles the JBD action after redefining the scalar field as $\Phi = \sqrt{\Psi}$. Finally, notice that, for a constant scalar field Φ, we have

$$S = \frac{\epsilon}{2}\int d^D x\sqrt{-g}R\Phi^2 \quad , \tag{2.67}$$

so that the Eintein-Hilbert action can be recovered if

$$\epsilon\Phi^2 = \kappa \rightarrow \Phi \propto \frac{1}{\sqrt{G}} \quad , \tag{2.68}$$

which was the motivation behind the Jordan-Brans-Dicken theory to explain gravity, *i.e.*, this theory relies on a local gravitational constant G. Given this relation between the Einstein and Jordan frame, we can change our perspective to say that, in order to go from one frame to another, a conformal transformation must be performed.

2.6 $f(R)$ Action

It is suggestive, from a phenomenological point of view, that, instead of a trivial linear contribution of the scalar curvature to the Lagrangian, one instead replaces it by a arbitrary function of it. In this class of modified theories of gravity known as $f(R)$ models, the action functional is written as

$$S_{f(R)} = \int d^4x\sqrt{-g}\left[\kappa f(R) + \mathcal{L}_m\right] \quad . \tag{2.69}$$

The variation of action functional with respect to the metric yields the modified field equation

$$2\kappa F(R)G_{\mu\nu} - \kappa[f(R) - RF(R)]g_{\mu\nu} = 2\kappa\Delta_{\mu\nu}F(R) + T_{\mu\nu} \quad , \tag{2.70}$$

where $F(R) \equiv df/dR$ and $\Delta_{\mu\nu} \equiv \nabla_\mu\nabla_\nu - g_{\mu\nu}\Box$. As expected, GR can be recovered by setting $f(R) = R$. Notice that the conservation of energy-momentum tensor is still obeyed.

Taking the trace of the last equation, we have

$$\kappa F(R)R - 2\kappa f(R) = 3\kappa\Box F(R) + T \quad , \tag{2.71}$$

so for a de Sitter expansion, $R = const$ and neglecting forms of matter $T = 0$, yields

$$F(R)R - 2f(R) = 0 \quad , \tag{2.72}$$

which has a trivial solution given by $f(R) = \alpha R^2$. This was first studied by Starobinsky as an inflationary model [14].

2.6.1 Equivalence Between $f(R)$ and Scalar Field Theory

In Section 2.5 we saw that a local conformal transformation of the Einstein-Hilbert action yields an equivalence between GR and a scalar field with a conformal coupling and JBD theories. In $f(R)$ models, this can also be ascertained (see, for example, Ref. [34]): following the literature in [13], we start by deducing the action in the Jordan's frame, which can be done by inserting an auxiliary scalar field in the action functional

$$S = \int d^4x\sqrt{-g}\left[\kappa(f(\chi) + f_{,\chi}\left(R-\chi\right)) + \mathcal{L}_m(g_{\mu\nu}, \Psi_m)\right] \quad , \tag{2.73}$$

where the Lagrangian density of matter not only depends on generic matter fields Ψ_m, but also on the metric. Variation with respect to the χ, yields the field equation

$$f_{,\chi\chi}(\chi)(R-\chi) = 0 \quad , \tag{2.74}$$

for $f_{,\chi\chi} = 0$, $R \neq \chi$, we recover the Einstein-Hilbert action with a constant contribution, since $f(\chi) = A + B\chi$ cancels out the linear scalar field contribution term. For $R = \chi$ and provided that $f_{,\chi\chi} \neq 0$, the action (2.69) is recovered. Defining the scalaron scalar field as

$$\psi = f_{,\chi}(\chi) \quad , \tag{2.75}$$

we write the action as

$$S = \int d^4x\sqrt{-g}\left[\kappa\psi R - U(\psi) + \mathcal{L}_m(g_{\mu\nu}, \Psi_m)\right] \quad , \tag{2.76}$$

where

$$U(\psi) = \kappa\left[\chi(\psi)\psi - f(\chi(\psi))\right] \quad , \tag{2.77}$$

the action above resembles the one in JBD theory without a kinetic term and an additional effective potential due to the scalaron: this is the so called O'Hanlon action [35].

We now transform the action to the Einstein frame, where the scalar curvature appears uncoupled. Performing a conformal transformation in the same fashion as (2.33) and inverting Eq. (2.55) for $D = 4$, we have

$$\begin{aligned} S = \int d^4x\sqrt{-\tilde{g}}\Big[\kappa\psi\Omega^{-2}\left(\tilde{R} + 6\frac{\tilde{\Box}\Omega}{\Omega} - 6\tilde{g}^{\mu\nu}\frac{\Omega_{,\mu}\Omega_{,\nu}}{\Omega^2}\right) - \\ \Omega^{-4}U + \Omega^{-4}\mathcal{L}_m(\Omega^{-2}\tilde{g}_{\mu\nu}, \Psi_m)\Big] \quad , \end{aligned} \tag{2.78}$$

defining our conformal factor as $\Omega^2 = \psi$ and redefining the scalaron through

$$\phi = \sqrt{3\kappa}\ln\psi = \sqrt{12\kappa}\ln\Omega \quad , \tag{2.79}$$

the action functional yields

$$S = \int d^4x\sqrt{-\tilde{g}}\left[\kappa\tilde{R} - \frac{1}{2}\tilde{g}^{\mu\nu}\phi_{,\mu}\phi_{,\nu} - V(\phi) + e^{\frac{-2\phi}{\sqrt{3\kappa}}}\mathcal{L}_m(e^{\frac{-\phi}{\sqrt{3\kappa}}}\tilde{g}_{\mu\nu}, \Psi_m)\right] \quad , \tag{2.80}$$

where

$$V(\phi) = \frac{U}{\psi^2} = \frac{\psi R - f}{\psi^2} \quad , \tag{2.81}$$

and the Lagrangian density of matter is accordingly affected by the conformal transformation of the metric: $\tilde{g}_{\mu\nu} = e^{\frac{\phi}{\sqrt{3\kappa}}}g_{\mu\nu}$.

In conclusion, for the class of $f(R)$ theories, the Einstein and Jordan frames are also equivalent, provided that we add an extra scalar field ϕ to the action functional.

Chapter 3

Non-Minimal Coupling Model

Having introduced the so-called $f(R)$ theories in the previous chapter, we now extend this proposal to include an arbitrary non-minimal coupling between curvature and matter.

3.1 Field Equations

For the purpose stated above, we opt for a Lagrangian density of the form

$$S = \int d^4x\sqrt{-g}\left[\kappa f_1(R) + f_2(R)\mathcal{L}_m\right] \quad . \tag{3.1}$$

The variation of the action with respect to the metric can be written as

$$\delta S = \int d^4x\left[f_2\delta\left(\sqrt{-g}\mathcal{L}_m\right) + \kappa\delta\sqrt{-g}f_1\right] + \int d^4x\sqrt{-g}\left[\kappa F_1 + F_2\mathcal{L}_m\right]\delta R \quad , \tag{3.2}$$

where, $F_i \equiv df_i/dR,\ (i = 1, 2)$. Taking into account that

$$\delta\sqrt{-g} = -\frac{1}{2}\sqrt{-g}g_{\mu\nu}\delta g^{\mu\nu} \quad , \tag{3.3}$$

$$\delta R = R_{\mu\nu}\delta g^{\mu\nu} - \Delta_{\mu\nu}\delta g^{\mu\nu} \quad , \tag{3.4}$$

$$T_{\mu\nu} = -\frac{2}{\sqrt{-g}}\frac{\delta\left(\sqrt{-g}\mathcal{L}_m\right)}{\delta g^{\mu\nu}} \quad , \tag{3.5}$$

the action can be written as

$$\begin{aligned}\delta S &= -\frac{1}{2}\int d^4x\sqrt{-g}\left[f_2T_{\mu\nu} + f_1g_{\mu\nu}\right]\delta g^{\mu\nu} \\ &+ \int d^4x\sqrt{-g}\left[\kappa F_1 + F_2\mathcal{L}_m\right]R_{\mu\nu}\delta g^{\mu\nu} \\ &- \int d^4x\sqrt{-g}\left[\kappa F_1 + F_2\mathcal{L}_m\right]\Delta_{\mu\nu}\delta g^{\mu\nu} \quad .\end{aligned} \tag{3.6}$$

Fixing the boundary of our manifold at infinity, integrating twice by parts the last contribution of (3.6), using Stoke's theorem and finally evoking the Principle of least action, we arrive at the field equation written below

$$2(\kappa F_1 + F_2\mathcal{L}_m)G_{\mu\nu} - [\kappa(f_1 - F_1 R) - F_2 R\mathcal{L}_m]g_{\mu\nu} = f_2 T_{\mu\nu} + 2\Delta_{\mu\nu}(\kappa F_1 + \mathcal{L}_m F_2) \quad (3.7)$$

Naturally, in the particular case $f_1 = R$, $f_2 = 1$, the above collapse to the Einstein field equations, while $f_1(R) = f(R)$, $f_2(R) = 1$ yields the equation of motion of $f(R)$ theories.

3.2 Non-Conservation of Energy-Momentum Tensor

One of the main features regarding the class of NMC theories is that the energy-momentum tensor may not be covariantly conserved. This can be seen by resorting to the Bianchi equation and the relation

$$(\Box\nabla^\nu - \nabla^\nu\Box)f = R_{\mu\nu}\nabla^\mu f \quad , \quad (3.8)$$

which arises by resorting to the definition of Riemann tensor. Applying it to Eq. (3.7) yields

$$\nabla_\mu T^{\mu\nu} = \frac{F_2}{f_2}(\mathcal{L}_m g^{\mu\nu} - T^{\mu\nu})\nabla_\mu R \quad , \quad (3.9)$$

which is clearly non conservative. Trivially, the conservation of the energy momentum tensor can be ascertained by considering a minimal coupling $f_2(R) = 1$. Other hypothesis come from constraining our Lagrangian density such that $\mathcal{L}_m g^{\mu\nu} = T^{\mu\nu}$; this, however, cannot be assumed for all matter types, and indeed this non-conservation is an intrinsic feature of the model [36]. From a cosmological perspective, the energy is conserved by taking the Lagrangian density of a perfect fluid, $\mathcal{L}_m = -\rho$ (see Ref. [37]).

Naturally, this non-conservation may imply that a test particle may deviate from its geodesic motion. To see this clearly, we resort to the energy-momentum tensor described in Eq. (2.16) and consider the projection operator

$$P_{\lambda\nu} = u_\lambda u_\nu + g_{\nu\lambda} \quad . \quad (3.10)$$

Contracting this tensor with Eq. (3.9) yields the modified geodesic equation

$$(\rho + p)u^\mu\nabla_\mu u_\lambda = -P_{\lambda\beta}p,^\beta + \frac{F_2}{f_2}\left(u_\lambda u^\alpha + \delta^\alpha_\lambda\right)\left(\mathcal{L}_m - p\right)R,_\alpha \quad , \quad (3.11)$$

which, can be written as, in a more natural form,

$$\frac{du_\lambda}{ds} - \Gamma^\sigma_{\mu\lambda} u^\mu u_\sigma = f_\lambda \quad , \tag{3.12}$$

where

$$f_\lambda = -P_{\lambda\beta}\frac{p^{,\beta}}{\rho + p} + \frac{F_2}{f_2}\left(u_\lambda u^\alpha + \delta^\alpha_\lambda\right)\frac{\mathcal{L}_m - p}{\rho + p} R_{,\alpha} \quad , \tag{3.13}$$

so that, besides the usual force imposed by the gradient pressure of the fluid, an extra contribution arises from the NMC. Notice that this extra contribution can be set to zero if the assumed matter type has a Lagrangian density $\mathcal{L}_m = p$. Finally, notice that this force is perpendicular to the flow direction of the fluid, *i.e.*, $f_\lambda u^\lambda = 0$.

3.3 Choice of the Lagrangian

As we can see in Eq. (3.7), the equations of motion on NMC theories explicitly depends on the Lagrangian density. In the perfect fluid scenario, this choice is not unique (see Refs. [37, 38]).

To see this clearly, we start by writing an EOS for the energy density, $\rho = \rho(n, s)$ as a function of the particle density n and the entropy per particle s under the identification of the First Law of Thermodynamics

$$d\rho = \mu dn + nTds \quad , \tag{3.14}$$

where μ is the chemical potential defined as

$$\mu \equiv \frac{\rho + p}{n} \quad . \tag{3.15}$$

Next, we introduce the flux vector of the particle density

$$J^\mu = \sqrt{-g} n u^\mu \quad , \tag{3.16}$$

which under the normalization $u^\mu u_\mu = -1$, allow us to define the particle density as $n = |J|/\sqrt{-g}$, with $|J| \equiv \sqrt{-g_{\mu\nu} J^\mu J^\nu}$. Finally, we write the action functional by inserting Lagrange coordinates α^A and spacetime scalars ϕ, θ and β_A in order to enforce constrains on the fluid's physical variables

$$S = \int d^4x [-\sqrt{-g}\rho(|J|/\sqrt{-g}, s) + J^\mu(\phi_{,\mu} + s\theta_{,\mu} + \beta_A \alpha^A_{,\mu})] \quad , \tag{3.17}$$

where the index A takes the values $1, 2, 3$. Taking into account the definition of the energy-momentum tensor

$$T_{\mu\nu} = \frac{-2}{\sqrt{-g}} \frac{\delta\left(\sqrt{-g}\mathcal{L}_m\right)}{\delta g^{\mu\nu}} \quad , \tag{3.18}$$

the variation with respect to the metric yields

$$T_{\mu\nu} = \rho u_\mu u_\nu + \left(n\frac{\partial\rho}{\partial n} - \rho\right)\left(g_{\mu\nu} + u_\mu u_\nu\right) \quad , \tag{3.19}$$

so that the pressure is defined as

$$p = n\frac{\partial\rho}{\partial n} - \rho \quad . \tag{3.20}$$

Direct computation show us that $\mu = \partial\rho/\partial n$, the usual definition for the chemical potential. The variation with respect to J^μ, ϕ, θ, s, α^A and β_A, yields the constrains

$$\frac{\delta S}{\delta J^\mu} = \mu u_\mu + \phi_{,\mu} + s\theta_{,\mu} + \beta_A \alpha^A_{,\mu} = 0 \quad , \tag{3.21}$$

$$\frac{\delta S}{\delta \phi} = -J^\mu_{\ ;\mu} = 0 \quad , \tag{3.22}$$

$$\frac{\delta S}{\delta \theta} = -(sJ^\mu)_{;\mu} = 0 \quad , \tag{3.23}$$

$$\frac{\delta S}{\delta s} = -\sqrt{-g}\frac{\partial\rho}{\partial s} + \theta_{,\mu}J^\mu = 0 \quad , \tag{3.24}$$

$$\frac{\delta S}{\delta \alpha^A} = -\left(\beta_A J^\mu\right)_{;\mu} = 0 \quad , \tag{3.25}$$

$$\frac{\delta S}{\delta \beta_A} = \alpha^A_{\ ,\mu} J^\mu = 0 \quad , \tag{3.26}$$

so that, for example, Eq. (3.22) states that the flux / particle density is conserved. Inspection of Eq. (3.24), show us that, after replacing the definition of density flux, we have

$$\frac{\partial\rho}{\partial s} = n\theta_{,\mu}u^\mu \quad , \tag{3.27}$$

since the temperature is related to the number of particles by

$$\frac{1}{n}\frac{\partial\rho}{\partial s}\Big|_n = T \quad , \tag{3.28}$$

the temperature may be alternatively defined with respect to the Lagrange multiplier θ as $T \equiv \theta_{,\mu}u^\mu$. Finally, notice that by solving Eq. (3.21) with respect to the 4-velocity and taking into the account the definition of the chemical potential (3.15), the action reduces to

$$S = \int d^4x\sqrt{-g}p \quad , \tag{3.29}$$

one of the standard choices of the Lagrangian density [39]. Notice that in order to obtain the constrains (3.21)-(3.26), the pressure must depend on the Lagrangian multipliers and the vector flux J^μ.

Now, the Lagrangian density that reproduces the Eq. (2.16) is not unique. Suppose that, instead of starting with the action functional described in Eq. (3.17), we started with

$$S = \int d^4x \left[-\sqrt{-g}\rho(n,s) - \phi J^\mu_{;\mu} - \theta(sJ^\mu)_{;\mu} - \alpha^A(\beta_A J^\mu)_{;\mu}\right] \quad , \tag{3.30}$$

noticing that the satisfy the constrains (3.21)-(3.26), the action functional reduces to

$$S = -\int d^4x\sqrt{-g}\rho(n,s) \quad , \tag{3.31}$$

which, again, reproduces the energy-momentum tensor of a perfect fluid. With this, we hence conclude that the Lagrangian choice is not unique, implying a degeneracy lift of it, which may yield different physical systems. Finally, although not discussed here, there is still, at least, another Lagrangian density which gives us the energy-momentum tensor of a perfect fluid, $\mathcal{L}_m = na$, where a is the physical free energy. Interestingly enough, it was shown that for a linear coupling between matter and geometry, the mass function of a star is strikingly similar regardless the Lagrangian density form (see Ref. [23]).

3.4 Equivalence Between NMC and Scalar Field Theory

By the same token as in GR and $f(R)$ theories, there is an equivalence between NMC and scalar field theory [40]. Due to the coupling between matter and geometry, we only need to notice that another scalar field must be introduced in the action functional

$$S = \int d^4x\sqrt{-g}\left[\kappa f_1(\chi) + \psi(R-\chi) + f_2(\chi)\mathcal{L}_m(g_{\mu\nu},\Psi_m)\right] \quad , \tag{3.32}$$

so that the actional functional in the Jordan frame can be written as

$$S = \int d^4x\sqrt{-g}\left[\psi R - V(\chi,\psi) - f_2(\chi)\mathcal{L}_m(g_{\mu\nu},\Psi_m)\right] \quad , \tag{3.33}$$

where

$$V(\chi,\psi) = \psi\chi - \kappa f_1(\chi) \quad , \tag{3.34}$$

with ψ and χ satisfying the field equations

$$\chi = R \quad , \tag{3.35}$$

$$\psi = \kappa F_1(\chi) + \mathcal{L} F_2(\chi) \quad . \tag{3.36}$$

The potential $V(\chi, \psi)$ can be seen as the interaction potential between these two fields. Equivalently, the Einstein frame can be recovered by performing the conformal transformation described in Section 2.6.1, which yields

$$\begin{aligned} S = \int d^4x \sqrt{-\tilde{g}} \Big[\Omega^{-2} \psi \left(\tilde{R} + 6 \frac{\tilde{\Box} \Omega}{\Omega} - 6 \tilde{g}^{\mu\nu} \frac{\Omega_{,\mu} \Omega_{,\nu}}{\Omega^2} \right) - \\ \Omega^{-4} \psi^2 U + \Omega^{-4} f_2(\chi) \mathcal{L}_m(\Omega^{-2} \tilde{g}_{\mu\nu}, \Psi_m) \Big] \quad , \end{aligned} \tag{3.37}$$

where $U \equiv \psi^{-2} V$. Defining

$$\psi = \Omega^2 \quad , \tag{3.38}$$

and

$$\phi = \sqrt{3\kappa} \ln \psi \quad , \tag{3.39}$$

we find that

$$S = \int d^4x \sqrt{-\tilde{g}} \left[\tilde{R} - \frac{1}{2\kappa} \tilde{g}^{\mu\nu} \phi_{,\mu} \phi_{,\nu} - U + e^{\frac{-2\phi}{\sqrt{3\kappa}}} f_2(\chi) \mathcal{L}_m(e^{\frac{-\phi}{\sqrt{3\kappa}}} \tilde{g}_{\mu\nu}, \Psi_m) \right] \quad , \tag{3.40}$$

where the metric in the Einstein frame is again related to the physical one by a scalar field: $\tilde{g}_{\mu\nu} = e^{\frac{\phi}{\sqrt{3\kappa}}} g_{\mu\nu}$.

Chapter 4

Relaxed Non-Minimally Coupled Regime

Having presented a brief introduction to the class of modified theory of gravity with a non-minimal coupling, we begin to develop the main work of this thesis. For that, we follow Refs. [31, 41], where it was shown that under a certain class of coupling functions, it is possible to mimic dark matter in the outer regions of galaxies with approximately spherical symmetry. For this, we impose that

$$\kappa F_1 + F_2 \mathcal{L}_m = \Omega\kappa \quad , \tag{4.1}$$

where Ω is a constant to be determined. This condition fixes what we call the relaxed regime for the NMC. Notice that this condition can be straightforwardly interpreted in the Jordan frame, by comparing it to Eq. (3.36) and setting $\psi = \Omega\kappa$.

This restriction can be seen as a fixed point condition, since the $\Delta_{\mu\nu}$ term on the field equations (3.7) vanishes accordingly. Indeed, in a cosmological context it was found that Eq. (4.1) arises naturally from a dynamical system formulation [42, 43], allowing for a de Sitter expansion of the Universe in the presence of a non-negligible matter content; a previous effort had shown that Eq. (4.1) leads to interesting modifications of the Friedmann equation [41] (see Ref. [19] for similar results).

In an astrophysical context, one can interpret it as a way to mimic dark matter [27, 31]. First used in Ref. [31], the above provides an immediate relation for $\rho = \rho(R)$ in the case of a pressureless dust distribution; that study also showed that numerical solutions to the overall field equations admit solutions that have very small oscillations around the latter.

Condition (4.1) acts as an additional constraint $R = R(\mathcal{L}_m)$ to the ensuing system of differential equations: as such, an extra equation of state (EOS) is no longer required

a priori: instead, one may in principle solve the full set of equations and then read the corresponding EOS parameter $\omega(\rho) = p(\rho)/\rho$ from it.

Inserting (4.1) into the field equations (3.7) leads to the simplified form

$$R_{\mu\nu} = \frac{1}{2\Omega\kappa}(f_2 T_{\mu\nu} + \kappa f_1 g_{\mu\nu}) \quad . \tag{4.2}$$

The ensuing trace yields

$$R = \frac{1}{2\Omega\kappa}\left(f_2 T + 4\kappa f_1\right) \quad , \tag{4.3}$$

so that solving it for f_1 and replacing into (4.2), one finally arrives at the traceless form

$$R_{\mu\nu} - \frac{1}{4}R g_{\mu\nu} = \frac{f_2}{2\Omega\kappa}\left(T_{\mu\nu} - \frac{1}{4}T g_{\mu\nu}\right) \quad , \tag{4.4}$$

which is strikingly similar to Unimodular gravity [44], although complemented by an NMC.

4.1 Dark Matter Mimicking

As we stated, the main objective of this work is to mimic dark matter through a NMC between curvature and visible matter. Given the relation $R = R(\mathcal{L}_m)$ that arises from the relaxed regime (4.1), we thus interprets the additional contributions to the field equations (4.4) as an effective dark matter: to ascertain this, we write the latter as the usual Einstein field equations with an additional energy-momentum tensor contribution for dark matter,

$$2\kappa G_{\mu\nu} = T^{(dm)}_{\mu\nu} + T_{\mu\nu} \quad . \tag{4.5}$$

Assuming that the latter also behaves as a perfect fluid,

$$T^{(dm)}_{\mu\nu} = (\rho_{dm} + p_{dm})v_\mu v_\nu + p_{dm} g_{\mu\nu} \quad , \tag{4.6}$$

with $v_\mu = u_\mu$ (so that this mimicked dark matter is "dragged" by visible matter), one can easily arrive at

$$\begin{aligned} p_{dm} &= \left(\frac{f_2}{\Omega} - 1\right)\omega\rho - \frac{f_2 T}{4\Omega} - \frac{\kappa R}{2} \quad , \\ \rho_{dm} &= \left(\frac{f_2}{\Omega} - 1\right)\rho + \frac{f_2 T}{4\Omega} + \frac{\kappa R}{2} \quad . \end{aligned} \tag{4.7}$$

In the case of GR, this component naturally vanishes due to the usual trace condition $R = -T/2\kappa$ and the minimal coupling $f_2(R) = 1$ (after imposing $\Omega = 1$).

4.2 Stationary Case

In this section we obtain a system of differential equations to our variables of interest. Assuming spherical symmetry and stationarity, we adopt the Birkhoff metric (2.15), here repeated for convenience:

$$ds^2 = -e^{2\phi(r)}dt^2 + e^{2\lambda(r)}dr^2 + r^2 d\Sigma^2 \quad . \tag{4.8}$$

The non-vanishing components of the energy-momentum tensor of matter (2.16) can be easily evaluated,

$$T_{tt} = \rho e^{2\phi}, \quad T_{rr} = p e^{2\lambda}, \quad T_{\theta\theta} = p r^2 \quad , \tag{4.9}$$

with trace $T = 3p - \rho$.

Given that a perfect fluid is described by a Lagrangian density $\mathcal{L} = -\rho$ [37, 38], while radiation obeys $\mathcal{L} = p$, we adopt the general description

$$\mathcal{L}_m = -\gamma\rho = \begin{cases} -\rho & , \gamma = 1 \\ p & , \gamma = -\omega \end{cases} \quad . \tag{4.10}$$

Taking the radial component of Eq. (3.9), we find

$$\phi'(\rho + p) = \frac{F_2}{f_2}(\mathcal{L}_m - p)R' - p' \quad . \tag{4.11}$$

Notice that the previous equation resembles Eq. (2.31), with the extra contribution due to the NMC. Replacing the form of the Lagrangian, we have

$$\phi' = -\beta\frac{F_2}{f_2}R' - \frac{1}{\omega + 1}\left(\omega' + \omega\frac{\rho'}{\rho}\right) \quad , \tag{4.12}$$

with the binary parameter

$$\beta = \frac{\gamma + \omega}{1 + \omega} = \begin{cases} 1 & , \gamma = 1 \\ 0 & , \gamma = -\omega \end{cases} \quad , \tag{4.13}$$

introduced for convenience.

We now address the field equation (4.4), resorting to the relation

$$g^{tt}R_{tt} - g^{rr}R_{rr} = -\frac{2}{r}e^{-2\lambda}\left(\phi' + \lambda'\right) \quad , \tag{4.14}$$

which, for the adopted diagonal metric, implies that

$$e^{-2\lambda}\left(\frac{\phi'+\lambda'}{r}\right)=\frac{\omega+1}{4\Omega\kappa}f_2\rho \quad . \tag{4.15}$$

The other independent component comes from taking $\theta-\theta$ in (4.4), which reads

$$\frac{e^{-2\lambda}}{r}\left(\lambda'-\phi'\right)-\frac{e^{-2\lambda}}{r^2}+\frac{1}{r^2}=\frac{R}{4}+\frac{\omega+1}{8\Omega\kappa}f_2\rho \quad . \tag{4.16}$$

Now, we solve Eq. (4.15) for $\lambda'(r)$ yielding

$$\lambda'=\frac{1+\omega}{4\Omega\kappa}f_2\rho e^{2\lambda}r-\phi' \quad . \tag{4.17}$$

Inserting this result into Eq. (4.16) allow us to define g_{rr} as

$$e^{2\lambda}=\frac{1+2r\phi'}{1-\frac{r^2}{4}\left(R-\frac{1+\omega}{2\Omega\kappa}f_2\rho\right)} \quad . \tag{4.18}$$

Taking into the account the expression for the scalar curvature

$$\frac{e^{2\lambda}}{2}R=\frac{e^{2\lambda}-1}{r^2}+\left(\frac{2}{r}+\phi'\right)\left(\lambda'-\phi'\right)-\phi'' \quad , \tag{4.19}$$

and replacing the two preceding expressions for $e^{2\lambda}$ and λ' into it we find that

$$\begin{aligned}&(1+2r\phi')\left[\frac{1+\omega}{2\Omega\kappa}f_2\rho\left(1+\frac{r}{2}\phi'\right)-\frac{R}{2}+\frac{1}{r^2}\right]= \\ &\left[\frac{1}{r^2}+\frac{4}{r}\phi'+2(\phi')^2+\phi''\right]\left[1-\frac{r^2}{4}\left(R-\frac{1+\omega}{2\Omega\kappa}f_2\rho\right)\right] \quad .\end{aligned} \tag{4.20}$$

Simplifying both sides, we can write the last equation as

$$\begin{aligned}\frac{R}{8} \quad &- \quad \frac{3}{8}\frac{1+\omega}{\Omega\kappa}f_2\rho r\left(\frac{1}{2r}+\phi'\right)+\frac{\phi'}{r}-\frac{1+\omega}{8\Omega\kappa}f_2\rho r^2\left((\phi')^2-\frac{\phi''}{2}\right) \\ &+ \quad \left(1-\frac{R}{4}r^2\right)\left((\phi')^2+\frac{\phi''}{2}\right)=0 \quad .\end{aligned} \tag{4.21}$$

Notice that, for consistency, one could obtain the same expression by differentiating Eq. (4.18) and inserting Eq. (4.17) into it.

Differentiating ϕ' with respect to the radial coordinate, yields

$$\begin{aligned}\phi'' \quad &= \quad \beta\left[\left(\frac{F_2}{f_2}\right)^2(R')^2-\frac{F_2'}{f_2}(R')^2-\frac{F_2}{f_2}R''\right]+\frac{\omega'}{(1+\omega)^2}\left[\omega'+\omega\frac{\rho'}{\rho}\right] \\ &- \quad \frac{1}{1+\omega}\left[\omega''+\omega'\frac{\rho'}{\rho}-\omega\left(\frac{\rho'}{\rho}\right)^2+\omega\frac{\rho''}{\rho}\right] \quad ,\end{aligned} \tag{4.22}$$

and replacing ϕ' and ϕ'' into Eq. (4.21), we finally arrive at the cumbersome expression below,

$$\begin{aligned}
& \frac{3}{8}\frac{1+\omega}{\Omega\kappa} f_2\rho r\left[\frac{1}{2r} - \beta\frac{F_2}{f_2}R' - \frac{1}{\omega+1}\left(\omega' + \omega\frac{\rho'}{\rho}\right)\right] + \frac{1}{r}\frac{1}{\omega+1}\left(\omega' + \omega\frac{\rho'}{\rho}\right) \\
+ \quad & \frac{\beta}{r}\frac{F_2}{f_2}R' + \frac{1+\omega}{8\Omega\kappa} f_2\rho r^2\left[\beta\left(\beta - \frac{1}{2}\right)\left(\frac{F_2}{f_2}\right)^2 (R')^2 + \frac{\beta}{2}\frac{F_2'}{f_2}(R')^2 + \frac{\beta}{2}\frac{F_2}{f_2}R''\right. \\
+ \quad & \frac{1}{2}\frac{\omega}{1+\omega}\frac{\rho''}{\rho} + \frac{1+4\omega}{2(1+\omega)^2}\frac{\rho'}{\rho}\omega' + \frac{(\omega')^2 + (1+\omega)\omega''}{2(1+\omega)^2} + \omega\frac{\omega-1}{2(\omega+1)^2}\left(\frac{\rho'}{\rho}\right)^2 \\
+ \quad & \left. 2\beta\frac{1}{1+\omega}\frac{F_2}{f_2}R'\left(\omega\frac{\rho'}{\rho} + \omega'\right)\right] - \left[1 - \frac{R}{4}r^2\right]\left[\beta\left(\beta + \frac{1}{2}\right)\left(\frac{F_2}{f_2}\right)^2 (R')^2\right. \\
- \quad & \frac{\beta}{2}\frac{F_2'}{f_2}(R')^2 - \frac{\beta}{2}\frac{F_2}{f_2}R'' + \omega\frac{3\omega+1}{2(\omega+1)^2}\left(\frac{\rho'}{\rho}\right)^2 + \frac{3(\omega')^2 - (1+\omega)\omega''}{2(1+\omega)^2} \\
- \quad & \left.\left. \frac{1}{2}\frac{\omega}{1+\omega}\frac{\rho''}{\rho} + \frac{4\omega-1}{2(1+\omega)^2}\omega'\frac{\rho'}{\rho} + 2\beta\frac{1}{1+\omega}\frac{F_2}{f_2}R'\left(\omega\frac{\rho'}{\rho} + \omega'\right)\right] - \frac{R}{8} = 0 \quad , \right. \qquad (4.23)
\end{aligned}$$

a second order and non-linear differential equation for three variables $\rho(r)$, $\omega(r)$ and $R(r)$.

4.3 Analytical Solution

We now aim to solve the above differential equation. First, we simplify it by defining the dimensionless variables

$$x \equiv r\sqrt{R_2} \quad , \quad y \equiv \frac{R}{R_2} \quad , \quad \varrho \equiv \frac{\rho}{2\kappa R_2} \quad , \qquad (4.24)$$

where R_2 is an as of yet arbitrary curvature scale that, as we shall see, equates with the characteristic curvature scale of the NMC. Given this, the relaxed regime condition (4.1) and trace Eq. (4.3) can be written as

$$\begin{aligned}
\Omega &= F_1 - 2\gamma F_2 R_2 \varrho \quad , \\
\Omega y &= f_2(3\omega - 1)\varrho + \frac{2f_1}{R_2} \quad ,
\end{aligned} \qquad (4.25)$$

while the differential equation (4.23) yields

$$
\begin{aligned}
& 3(1+\omega)\frac{f_2\varrho}{\Omega}x\left[\frac{1}{x}-2\beta\frac{F_2R_2}{f_2}y'-\frac{2}{\omega+1}\left(\omega'+\omega\frac{\varrho'}{\varrho}\right)\right]+\frac{8\beta}{x}\frac{F_2R_2}{f_2}y' \\
+ \quad & \frac{8}{x}\frac{1}{\omega+1}\left(\omega'+\omega\frac{\varrho'}{\varrho}\right)+(1+\omega)\frac{f_2\varrho}{\Omega}x^2\left[\beta\left(2\beta-1\right)\left(\frac{F_2R_2}{f_2}\right)^2(y')^2\right. \\
+ \quad & \beta\frac{F_2'R_2^2}{f_2}(y')^2+\beta\frac{F_2R_2}{f_2}y''+\frac{(\omega')^2+(1+\omega)\omega''}{(1+\omega)^2}+\omega\frac{\omega-1}{(\omega+1)^2}\left(\frac{\varrho'}{\varrho}\right)^2 \\
+ \quad & \left.\frac{\omega}{1+\omega}\frac{\varrho''}{\varrho}+\frac{1+4\omega}{(1+\omega)^2}\frac{\varrho'}{\varrho}\omega'+4\beta\frac{1}{1+\omega}\frac{F_2R_2}{f_2}y'\left(\omega\frac{\varrho'}{\varrho}+\omega'\right)\right] \\
- \quad & \left[4-yx^2\right]\left[\beta\left(2\beta+1\right)\left(\frac{F_2R_2}{f_2}\right)^2(y')^2-\beta\frac{F_2'R_2^2}{f_2}(y')^2-\beta\frac{F_2R_2}{f_2}y''\right. \\
+ \quad & \frac{3(\omega')^2-(1+\omega)\omega''}{(1+\omega)^2}+\omega\frac{3\omega+1}{(\omega+1)^2}\left(\frac{\varrho'}{\varrho}\right)^2-\frac{\omega}{1+\omega}\frac{\varrho''}{\varrho}+\frac{4\omega-1}{(1+\omega)^2}\omega'\frac{\varrho'}{\varrho} \\
+ \quad & \left.4\beta\frac{1}{1+\omega}\frac{F_2R_2}{f_2}y'\left(\omega\frac{\varrho'}{\varrho}+\omega'\right)\right]-y=0 \quad . \qquad (4.26)
\end{aligned}
$$

where the derivatives are now with respect to x. In order to proceed with our calculations, we need to give explicit expressions to $f_i(R)$. Following Ref. [31], we assume a trivial $f_1(R)$ and a power law for the NMC of the form

$$
\begin{aligned}
f_1(R) &= R \quad , \\
f_2(R) &= 1+\left(\frac{R}{R_2}\right)^n \quad , \qquad (4.27)
\end{aligned}
$$

where R_2 is a characteristic curvature scale. With the choice of the Lagrangian density of a perfect fluid $\mathcal{L}_m=-\rho \to \gamma=1$, conditions (4.25) read

$$
\begin{aligned}
\frac{1-\Omega}{2n}y^{1-n} &= \varrho \quad , \qquad (4.28) \\
(\Omega-2)y &= (1+y^n)(3\omega-1)\varrho \quad .
\end{aligned}
$$

Regarding the fixed point condition, in Ref. [31] it was found that the energy density and curvature were related by

$$
R=\frac{1-2n}{2\kappa}\left(\frac{R}{R_2}\right)^n\rho \quad , \qquad (4.29)
$$

which, written in terms of the dimensionless variables (4.24), reads

$$
\frac{1}{1-2n}y^{1-n}=\varrho \quad . \qquad (4.30)
$$

Matching both results, we fix our constant Ω as

$$\Omega = \frac{1-4n}{1-2n} \quad . \tag{4.31}$$

With this, the conditions above translate into

$$\begin{aligned} y^{1-n} &= (1-2n)\varrho \quad , \\ y &= (1-2n)(1+y^n)(1-3\omega)\varrho \quad . \end{aligned} \tag{4.32}$$

Furthermore, notice that the set of relations

$$\begin{aligned} f_2 &= 1+y^n \quad , \\ \frac{F_2 R_2}{f_2} &= n\frac{y^{n-1}}{1+y^n} \quad , \\ \frac{F_2' R_2^2}{f_2} &= n(n-1)\frac{y^{n-2}}{1+y^n} \quad , \end{aligned} \tag{4.33}$$

are only dependent on the power law exponent n.

We are finally in position to solve our differential equation under the appropriate conditions. For that purpose, we notice that visible matter is non-relativistic, so that the EOS parameter should be small, $\omega \sim 0$. With this condition, solving the trace in Eq. (4.32) for the EOS parameter yields

$$y^n = (1+y^n)(1-3\omega)y^{1-n} \rightarrow y^n = \frac{1}{3\omega} - 1 \sim \frac{1}{3\omega} \quad , \tag{4.34}$$

so that the vanishingly small pressure of visible matter translates into the dominance of the NMC term, $\omega \sim 0 \rightarrow y^n \sim f_2 \gg 1$; since we consider a negative exponent $n < 0$, this translates into a very small reduced curvature $y \ll 1$.

Given this, the visible matter density ρ and EOS parameter ω are written implicitly in terms of the scalar curvature as

$$\rho = \frac{2\kappa R_2}{1-2n}\left(\frac{R}{R_2}\right)^{1-n} \quad , \quad \omega = \frac{1}{3}\left(\frac{R}{R_2}\right)^{-n} \quad , \tag{4.35}$$

while the mimicked dark matter distribution are given by direct computation of Eqs. (4.7) after replacing the expressions above and the f_i functions in (4.27)

$$\begin{aligned} \rho_{dm} &\sim \frac{1-n}{1-4n} 2\kappa R \quad , \\ p_{dm} &\sim \frac{n}{1-4n} 2\kappa R \quad , \end{aligned} \tag{4.36}$$

where we neglected the extra contributions which arise from the fluid's pressure, which are clearly perturbative by Eq. (4.35).

Given the low-curvature regime above, we attempt to solve the differential equation (4.26) by resorting to the algebraic relations (4.32), (4.33) and (4.34). To do so, we first solve it for y'' and expand (4.26) perturbatively $y \sim 0$ to first order, yielding the considerably simplified equation

$$-\frac{2y'(x)}{x} + (1+2n)\frac{y'(x)^2}{y(x)} - y''(x) = 0 \quad . \tag{4.37}$$

This non-linear second order differential equation has an analytical solution given by

$$y(x) = y_f \left(\frac{2x}{x_f + x}\right)^{\frac{1}{2n}} \quad , \tag{4.38}$$

where x_f and y_f are integration constants: it is easy to check that $y(x_f) = y_f$, so this normalization simply gives us the value of the scalar curvature evaluated at a given radius; we choose to identify x_f as the reduced radius of the visible part of a given galaxy, while y_f the correspondent value of the reduced scalar curvature.

In the asymptotic regime $x \gg x_f$, *i.e.* for a region sufficiently far away from our galaxy, one has

$$y(x) \sim 2^{\frac{1}{2n}} y_f \left(1 - \frac{1}{2n}\frac{x_f}{x}\right) \quad , \tag{4.39}$$

so that the scalar curvature approaches the value

$$y(\infty) \sim 2^{\frac{1}{2n}} y_f \quad , \tag{4.40}$$

which we interpret as the background contribution of the curvature.

Conversely, in the limit $x \ll x_f$, *i.e.* for regions where we aim to obtain a mimicked dark matter halo, one has

$$y(x) \sim y_f \left(\frac{2x}{x_f}\right)^{\frac{1}{2n}} \quad . \tag{4.41}$$

The scalar curvature and the respective dark matter contributions can be explicitly written as

$$\begin{aligned} R(r) &= R_f \left(\frac{2r}{r_f + r}\right)^{\frac{1}{2n}} \quad , \\ \rho_{dm}(r) &= \frac{1-n}{1-4n} 2\kappa R_f \left(\frac{2r}{r_f + r}\right)^{\frac{1}{2n}} \quad , \\ p_{dm}(r) &= \frac{n}{1-4n} 2\kappa R_f \left(\frac{2r}{r_f + r}\right)^{\frac{1}{2n}} \quad , \end{aligned} \tag{4.42}$$

while visible matter is characterized by

$$\begin{aligned} \rho(r) &= \frac{2\kappa R_f}{1-4n}\left(\frac{R_f}{R_2}\right)^{-n}\left(\frac{2r}{r_f+r}\right)^{\frac{1-n}{2n}} \quad , \\ \omega(r) &= \frac{1}{3\sqrt{2}}\left(\frac{R_f}{R_2}\right)^{-n}\sqrt{1+\frac{r_f}{r}} \quad , \end{aligned} \tag{4.43}$$

where r_f denotes a given boundary radius of the galaxy and R_f the correspondent scalar curvature.

Chapter 5

Matter Profiles and Constrains to the Model

In the previous chapter, we obtained an exact solution to the mimicked dark matter profile for the halo region of a given galaxy. With this in mind, we now aim to compare this solution with the standard profiles which can be found in the literature. Also, we show that the energy conditions are satisfied under the appropriate range of values for the power law exponent n. Finally, constraints to the non-minimal coupling parameter will be given.

5.1 Standard Matter Profiles

Given the dark and visible matter energy density solutions, we start this new chapter by comparing our solutions with the profiles of interest, namely the Hernquist, Navarro-Frenk-White (NFW) [45] and isothermal [46] distributions. For that, we start by noting that away from the boundary of the galaxy, $r \ll r_f$ and we can use (4.42) to write

$$\rho_{dm}(r) \sim \frac{1-n}{1-4n} 2\kappa R_f \left(\frac{2r}{r_f}\right)^{\frac{1}{2n}} \quad . \tag{5.1}$$

Thus, we obtain a direct translation between the slope of the dark matter distribution ρ_{dm} and the NMC exponent n. By the same token, the visible profile can also be approximated in Eq. (4.43) by

$$\rho(r) \sim \frac{2\kappa R_f}{1-4n} \left(\frac{R_f}{R_2}\right)^{-n} \left(\frac{2r}{r_f}\right)^{\frac{1-n}{2n}} \quad . \tag{5.2}$$

5.1.1 Cusped Profiles

Along the years, an exhaustive attempt to theoretically find density profiles which describe dark matter has been pursued. Through N-body simulations and spectrography, it was found that most models fit in a empirical density model, the so called cusped profile [47]

$$\rho(r) = \frac{\rho_{cp}}{\left(\frac{r}{a}\right)^{\gamma}\left(1+\frac{r}{a}\right)^{m-\gamma}} \quad , \tag{5.3}$$

where ρ_{cp} denotes the density scale, a the transition radius between visible and dark matter dominance and γ, m the inner and outer logarithmic slopes, respectively. This profiles can model not only dark matter, but also the density profile of visible matter.

To determine the correspondent mass profile for the outer region, we start by taking $r \gg a$ in (5.3),

$$\rho(r) \sim \rho_{cp}\left(\frac{a}{r}\right)^{m} \quad , \tag{5.4}$$

notice that the density is independent of the inner slope γ. Resorting to Eq. (2.27), the mass profile is given by

$$M(r) = \frac{4\pi}{3-m} a^{m} \rho_{cp} r^{3-m} \quad , \tag{5.5}$$

for $m \neq 3$.

To determine the rotational velocity, we invoke Newton's law of gravitation and find that

$$v^2 = \frac{GM(r)}{r} = \frac{4\pi}{3-m} a^{m} \rho_{cp} r^{2-m} \quad . \tag{5.6}$$

We thus see that the outer logarithmic slope m regulates the asymptotic behavior of the rotation curve, which is flat if $m = 2$, while different values of m translate into a increasing or decreasing behavior, for $m < 2$ or $m > 2$, respectively.

5.1.2 Hernquist Visible Matter Profile

Historically, one of the outstanding candidates for density profile of visible matter is the well known Hernquist profile [48],

$$\rho_{Hernq}(r) = \frac{M}{2\pi a^3} \frac{1}{\frac{r}{a}\left(1+\frac{r}{a}\right)^3} \quad , \tag{5.7}$$

which was initially introduced to solve the luminosity problem for elliptical galaxies. In the previous equation, M denotes the total visible mass of a given galaxy. Comparing

with the cusped profile, this is the particular case where $\gamma = 1,\ m = 4$ and $\rho_{cp} = M/(2\pi a^3)$.

For the inner and outer regions, *i.e.,* $r \ll a$ and $r \gg a$, respectively, one has

$$\rho_{Hern}(r) \sim \frac{M}{2\pi a^3} \begin{cases} \frac{a}{r} \ , & r \ll a \\ \left(\frac{a}{r}\right)^4 \ , & r \gg a \end{cases} \ , \tag{5.8}$$

so that comparing the outer region limit with Eq. (5.2), it is trivial to check that this is realized by setting the NMC exponent $n_{Hernq} = -1/7$.

Resorting to Eq. (5.1), the correspondent DM profile translates into

$$\rho_{dm} = \frac{16\kappa R_f}{11} \left(\frac{2r}{r_f}\right)^{-\frac{7}{2}} \ . \tag{5.9}$$

5.1.3 Navarro-Frenk-White Dark Matter Profile

Regarding dark matter density profiles, the first one considered here is the Navarro-Frenk-White [45], which was introduced *a priori* in order to study N-body simulations of dark matter halo in galaxies. It is given by

$$\rho_{NFW}(r) = \frac{\rho_{cp}}{\frac{r}{a}\left(1+\frac{r}{a}\right)^2} \ , \tag{5.10}$$

and is a cusped profile with $\gamma = 1, m = 3$. Following the same procedure as before, we have that

$$\rho_{NFW}(r) \sim \rho_{cp} \begin{cases} \frac{a}{r} \ , & r \ll a \\ \left(\frac{a}{r}\right)^3 \ , & r \gg a \end{cases} \ , \tag{5.11}$$

comparing with (5.1), we find that $n_{NFW} = -1/6$. Resorting to Eq. (5.2), the density profile of visible matter translates into

$$\rho(r) \sim \frac{6\kappa R_f}{5} \left(\frac{R_f}{R_2}\right)^{1/6} \left(\frac{2r}{r_f}\right)^{-7/2} \ . \tag{5.12}$$

5.1.4 Isothermal Dark Matter Profile

Finally, we have the isothermal profile, which is also used to model dark matter behavior in the outer regions. Mathematically, this can be obtained by considering a polytropic equation of state $p = K\rho$ and solving the hydrostatic equilibrium equation

$$\frac{d\Phi}{dr} = -\frac{1}{\rho}\frac{dp}{dr} \ , \tag{5.13}$$

where $\Phi \equiv \Phi(r)$ is the gravitational potential. Solving it for ρ, one has

$$\rho_I(r) = \frac{v_\infty^2}{2\pi G r^2} \quad . \tag{5.14}$$

It is a cusped profile with $m = \gamma = 2$, and the divergence at $r = 0$ leads it to being called the singular isothermal profile, where v_∞ is the asymptotically velocity, *i.e.,* the (constant) velocity for outer regions with the correspondence $v_\infty^2 = 2\pi G \rho_{cp} a^2$.

By the same token as before, one finds $n_I = -1/4$ and the correspondent visible density profile

$$\rho(r) = \kappa R_f \left(\frac{R_f}{R_2}\right)^{1/4} \left(\frac{2r}{r_f}\right)^{-5/2} \quad . \tag{5.15}$$

Finally, we summarize the characteristic behaviors for both dark and visible matter density in Table. 5.1

Profiles	n	$\rho(r)$	$\rho_{dm}(r)$
Hernquist	$-1/7$	r^{-4}	$r^{-7/2}$
NFW	$-1/6$	$r^{-7/2}$	r^{-3}
Isothermal	$-1/4$	$r^{-5/2}$	r^{-2}

Table 5.1: Outer region behavior for the relevant profiles

To complete our discussion, we introduce some alternative models, such as the Burkert profile [49]

$$\rho_B(r) = \rho_v \frac{a^3}{(r+a)(r+a)^2} \quad , \tag{5.16}$$

where $\rho_v = \rho(0)$, thus removing the core singularity. Notice that it resembles the NFW profile for the outer regions ($\rho \sim r^{-3}$). With a different family of functions we have the Einasto profile

$$\rho(r) = \rho_v \exp\left[-d_p \left(\left[\frac{r}{a}\right]^{1/p} - 1\right)\right] \quad , \tag{5.17}$$

where d_p is an adequate function of p, such that $r = a$ encloses half of the total mass; and the deprojected Sérsic law

$$\rho(r) = \rho_v \left(\frac{r}{a}\right)^{-p_m} \exp\left[-d_m \left(\frac{r}{a}\right)^{\frac{1}{m}}\right] \quad , \tag{5.18}$$

with p_m and d_m characteristic scales.

5.2 Mass Budget

Since in Section 4.1 we imposed that the total contribution of dark and visible matter to the energy momentum tensor satisfies the GR equation, we can simply cast the metric elements which were found in Section 2.3,

$$\begin{aligned} m(r) &= 4\pi \int \rho_t(r) r^2 dr \quad , \\ e^{2\lambda(r)} &= \left(1 - \frac{m(r)}{8\pi\kappa r}\right)^{-1} \quad , \\ e^{2\phi(r)} &= \exp\left(\int \frac{4\pi p_t(r) r^3 + m(r)}{r(8\pi\kappa r - m(r))} dr\right) \quad , \end{aligned} \tag{5.19}$$

where ρ_t and p_t denote, respectively, the total (visible + dark) energy density and pressure. Regarding this, notice that we could always find the metric elements by using the expressions found in Section 4.2: however, the above is clearly more convenient, once the mimicked dark matter behavior has been written explicitly. Furthermore, it is known that a galaxy is within the validity of the Newtonian regime, $g^{\mu\nu} \sim \eta^{\mu\nu}$.

5.2.1 Mass

When computing the mass of our spherical object, one needs to be careful with the limits of integration: indeed, since the validity of our solution (4.38) is satisfied only in the halo regions of our galaxy, we cannot simply integrate it from the center to a given radius r. Hence, we define an inner radius a, in the same sense described in Section 5.1.1, *i.e.,* the transition radius between dark and visible matter dominance.

Using the definition of mass in the first equation (5.19), one has that the mass component M_i enclosed in the halo region $a < r < r_f$ is given by

$$M_i = 4\pi \int_a^{r_f} \rho_i(r) r^2 dr \quad . \tag{5.20}$$

Resorting once more to Eqs. (5.1) and (5.2)

$$\begin{aligned} \rho(r) &\sim \frac{1}{1-4n} 2\kappa R_2 \left(\frac{R_f}{R_2}\right)^{1-n} \left(\frac{2r}{r_f}\right)^{\frac{1-n}{2n}} \quad , \\ \rho_{dm}(r) &\sim \frac{1-n}{1-4n} 2\kappa R_f \left(\frac{2r}{r_f}\right)^{\frac{1}{2n}} \quad , \end{aligned} \tag{5.21}$$

we find the contribution of dark matter mass to the galaxy halo,

$$M_{dm} = h_n \frac{R_f r_f^3 c^2}{G} \left[1 - \left(\frac{a}{r_f}\right)^{\frac{1+6n}{2n}}\right] \quad , \tag{5.22}$$

for $n \neq -1/6$, where

$$h_n \equiv \frac{2^{\frac{1}{2n}} n(1-n)}{(1-4n)(1+6n)} \quad . \tag{5.23}$$

Notice that in order to keep the mass positive defined, the condition $n < -1/6$ is required.

For $n = -1/6$, it is easy to see that the dark matter mass has a logarithmic dependence

$$M_{dm} = \frac{7}{160} R_f r_f^2 \frac{r_f c^2}{G} \ln\left(\frac{r_f}{a}\right) \quad . \tag{5.24}$$

For any value of the exponent $n \neq -1/5$ (which does not correspond to any profile of interest and is thus disregarded), the visible mass enclosed within the mimicked dark matter halo is given by

$$M_v = h'_n \left(\frac{R_f}{R_2}\right)^{-n} \frac{R_f r_f^3 c^2}{G} \left[1 - \left(\frac{a}{r_f}\right)^{\frac{5n+1}{2n}}\right] \quad , \tag{5.25}$$

with

$$h'_n \equiv \frac{2^{\frac{1-n}{2n}} n}{(1-4n)(1+5n)} \quad . \tag{5.26}$$

The ratio between dark matter and visible mass is thus

$$\frac{M_{dm}}{M_v} = \frac{h_n}{h'_n} \left(\frac{R_f}{R_2}\right)^n \frac{1 - \left(\frac{a}{r_f}\right)^{\frac{1+6n}{2n}}}{1 - \left(\frac{a}{r_f}\right)^{\frac{1+5n}{2n}}} \quad , \tag{5.27}$$

for $n \neq -1/6$ and

$$\frac{M_{dm}}{M_v} = \frac{7}{6\sqrt{2}} \left(\frac{R_2}{R_f}\right)^{1/6} \frac{\ln\left(\frac{r_f}{a}\right)}{\sqrt{\frac{r_f}{a} - 1}} \quad , \tag{5.28}$$

for $n = -1/6$. Since $h'_n \sim h_n$ and $a \lesssim r_f$, the low-curvature regime $(R_f/R_2)^n \gg 1$ implies that dark matter mass will dominate, as desired.

5.3 Energy Conditions

In this section, we focus our attention in the energy conditions. These can be obtained by considering the Raychaudhuri equation in the case of a congruence of null geodesics defined by a vector field k^μ by (see, for example, Refs. [28, 50])

$$\frac{d\theta}{d\tau} = -\frac{1}{2}\theta^2 - \sigma_{\mu\nu}\sigma^{\mu\nu} + \omega_{\mu\nu}\omega^{\mu\nu} - R_{\mu\nu}k^\mu k^\nu \quad , \tag{5.29}$$

where θ is the expansion parameter, $\sigma_{\mu\nu}$ the shear and $\omega_{\mu\nu}$ the rotation associated with the congruence. This equation can describe, for instance, the change of volume of a given ball for a co-moving observer in the center of it. Gravity remains attractive as long as the variation of θ with respect to the proper time τ stays negative.

Since we interpret our model as equivalent to GR with the effect of the NMC ascribed to an additional, effective, component that behaves as a perfect fluid, the strong, null, weak and dominant energy conditions can be cast, respectively, as

$$\begin{cases} \rho_t + 3p_t \geq 0 & , \text{ SEC} \\ \rho_t + p_t \geq 0 & , \text{ NEC} \\ \rho_t \geq 0 & , \text{ WEC} \\ \rho_t \geq p_t \geq -\rho_t & , \text{ DEC} \end{cases} . \tag{5.30}$$

In here, ρ_t and p_t denote the total (visible + dark) energy density and pressure. Since the low-curvature regimes induces a zero pressure and a perturbative energy density, we can safely neglect both contributions.

Considering the dark matter components in Eq. (4.36), the SEC, NEC and WEC can be summarized as

$$\left(\frac{1-2n}{1-4n}\right)(1+E_n)\,\rho \geq 0 \quad , \tag{5.31}$$

where

$$E_n = \begin{cases} 2n & , \text{ SEC} \\ 0 & , \text{ NEC} \\ -n & , \text{ WEC} \end{cases} , \tag{5.32}$$

while the DEC is satisfied if

$$0 \geq \left(\frac{1-2n}{1-4n}\right)(2n-1) \geq 2\left(\frac{1-2n}{1-4n}\right)(n-1) \quad . \tag{5.33}$$

Thus, the SEC is satisfied for $-1/2 \leq n < 1/4$, while the NEC, WEC and DEC are satisfied for $n < 1/4$, which encompasses all the relevant visible and dark matter profiles considered here.

5.4 Model Parameter Constraints

In this section, we aim to compare the expressions found in the section 5.2.1 with observed values. Since our solutions were found by the assumption that our object

has spherical symmetry, we adopt the dataset reported in Refs. [51, 52] for galaxies of type E0, which display low eccentricity. The relevant quantities (a, r_f) and enclosed visible and dark matter masses (as inferred from the corresponding rotation curves) are depicted in Table 5.2.

NGC	$M_v(10^{10}M_\odot)$	$M_{dm}(10^{11}M_\odot)$	$r_f(kpc)$	$a(kpc)$	$y_f(10^{-3})$
2434	4.6	1.9	18	5.1	0.6
5846	36.4	8.5	70	21.1	2.1
6703	5.6	1.2	18	2.7	1.1
7145	3.8	1.4	25	4.0	0.4
7192	7.1	2.7	30	4.1	0.3
7507	7.9	3.5	18	4.7	0.3
7626	30.7	8.7	50	11.0	0.4

Table 5.2: Data obtained by performing a fit to rotational curves of galaxies.

Following this, a χ^2 fitting procedure is followed to ascertain which parameters n and R_2 lead to the best fit of the mimicked dark matter to visible mass ratio (5.27) and (5.28) to the values obtained from Table 5.2. For that purpose, one eliminates R_f in this equations by resorting to (5.22) and (5.24) yielding, respectively

$$\frac{M_{dm}}{M_v} = \frac{h_n^{1-n}}{h_n'}\left(r_f^2 R_2 \frac{r_f c^2}{GM_{dm}}\right)^{-n}\left[1-\left(\frac{a}{r_f}\right)^{\frac{5n+1}{2n}}\right]^{-1}\left[1-\left(\frac{a}{r_f}\right)^{\frac{6n+1}{2n}}\right]^{1-n}, \quad (5.34)$$

for $n \neq -1/6$, and

$$\frac{M_{dm}}{M_v} = \frac{7}{12}\left(\frac{7}{20}\frac{r_f c^2}{GM_{dm}} r_f^2 R_2\right)^{1/6} \frac{\left[\ln\left(\frac{r_f}{a}\right)\right]^{7/6}}{\sqrt{\frac{r_f}{a}-1}}, \quad (5.35)$$

for $n = -1/6$. Following through with the numerical session, it is found that the value for the adjusted correlation coefficient r^2 increases as we arbitrarily approach $n = -1/6$. The best fit is then found when $n = -1/6$, yielding a correlation coefficient $r^2 = 0.86$: this relatively low value can be reflected by small deviations from sphericity in the selected type E0 galaxies, as well as unmodeled localized features and inhomogeneities. The best fit for the characteristic length scale was found to be $R_2 \approx 5\ \mathrm{Mpc}^{-2}$, although with a large uncertainty stemming from the relative lack of sensitivity of (5.35) to it: as such, we are only allowed to conclude that $R_2 \sim \mathrm{Mpc}^{-2}$.

Finally, it is also interesting to see where the assumption behind the low-curvature regime holds. For that, one resort to Eqs. (5.27) and (5.28) and solve it for R_f/R_2.

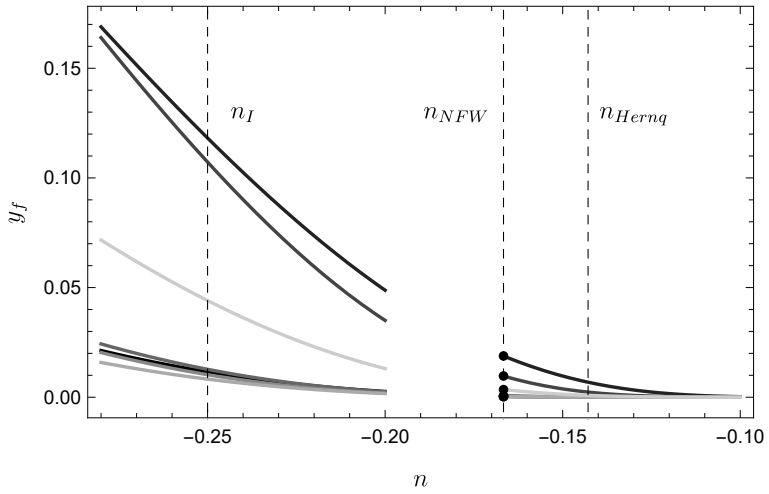

Figure 5.1: Plot of the low-curvature regime validation as a function of the power law exponent n.

This yields

$$y_f = \left(\frac{M_{dm}}{M_v}\right)^{\frac{1}{n}} \left(\frac{h'_n}{h_n}\right)^{\frac{1}{n}} \left(\frac{1-\left(\frac{a}{r_f}\right)^{\frac{1+5n}{2n}}}{1-\left(\frac{a}{r_f}\right)^{\frac{1+6n}{2n}}}\right)^{\frac{1}{n}} , \tag{5.36}$$

for $n \neq -1/6$, and

$$y_f = \left(\frac{7}{6\sqrt{2}}\right)^6 \left(\frac{M_v}{M_{dm}}\right)^6 \left(\frac{\ln\left(\frac{r_f}{a}\right)}{\sqrt{\frac{r_f}{a}}-1}\right)^6 , \tag{5.37}$$

for $n = -1/6$.

Focusing on Fig. 5.1, we see that the regime holds for the power law exponents identified with the standard density profiles. However, as n decreases, the fitted curves of each galaxy, which are representative of Eq. (5.36) tend to break the regime. The black dots represents the different NGC galaxies for n_{NFW}, where the values of y_f are given in the last column of Table 5.2, which are clearly perturbative.

Chapter 6

Conclusions

In this thesis, we showed that the rich phenomenology of a model endowed with a non-minimal coupling between curvature and matter allows for the possibility of mimicking dark matter profiles for galaxies which exhibit spheric symmetry. This result was obtained by assuming a relaxed regime, interpreted as a fixed point condition, which allowed us to relate the Lagrangian density with the curvature, with no need for an additional EOS.

By assuming a power law form to the NMC function $f_2(R)$ (motivated by the previous work found in Ref. [31]), we solved the relevant equations in the perturbative regime and characterized the ensuing solutions: in particular, we confirmed the relation between visible and dark matter density profiles found in that study and further refined it by explicitly deriving their individual dependence on the exponent n of the NMC function: we recall that Ref. [31] only provide the translation between visible and dark matter profiles, but did not account for why these adopt a particular radial dependence.

We also showed that the NMC must be strong, $f_2 \gg 1$ if the mimicked dark matter is to dominate at large distances: this translates into a perturbative regime where the scalar curvature is much smaller than the characteristic curvature scale $R \ll R_2$. Furthermore, we showed that this condition does not violate the appropriate energy conditions.

Finally, the enclosed masses were obtained and used to compare with observation, showing that the NFW profile for the mimicked dark matter component is favored, given by an exponent $n_{NFW} = -1/6$ (or an arbitrarily close value). The characteristic curvature scale was found to be of the order of $R_2 \sim 1$ Mpc^{-2}, although the quality of the fit is not sufficient to fix it more accurately.

Given the interesting results obtained, it is tempting to assume that all dark matter can be regarded as due to the dynamical effect of the NMC between curvature and matter. However, the striking evidence of the separation between dark and visible matter provided by the Bullet cluster further complicates the issue [8]: indeed, if dark

matter is not a real matter type, but merely reflects the enhanced gravity of visible matter due to the model under scrutiny (or, indeed, any extension of GR), then it is plausible that it should inherit the spatial symmetry of visible matter: in other words, if visible matter interacts and produces the shock wave directly observed in the Bullet cluster, the ensuing gravitational profile should also exhibit this feature, instead of maintaining an approximate spherical symmetry. This, however, could be tackled by assuming that the NMC is more strongly coupled to neutrinos, which do not interact, than to visible matter: such possibility should be further investigated.

Bibliography

[1] A. Silva and J. Páramos, arXiv:1703.10033v2 [gr-qc] .

[2] C. M. Will, *Living Rev. Rel.* **9**, 3 (2006).

[3] O. Bertolami and J. Páramos, "The experimental status of Special and General Relativity", in *Handbook of Spacetime*, Springer, Berlin (2013).

[4] LIGO Scientific Collaboration and Virgo Collaboration, *Phys. Rev. Lett.* **116**, 061102 (2016).

[5] E. J. Copeland, M. Sami and S. Tsujikawa, *Int. J. Mod. Phys.* D **15**, 1753 (2006).

[6] S. Weinberg, *Rev. Mod. Phys.* **61**, 1 (1989).

[7] G. Bertone, D. Hooper and J. Silk, *Phys. Repts.* **405**, 279 (2005).

[8] D. Clowe, A. Gonzalez and M. Markevitch *Ap. J.* **604**, 2 (2004).

[9] M. Milgrom, *Ap. J.* **270**, 365-370 (1983).

[10] O. Bertolami and J. Páramos, [arXiv:gr-qc/0611025].

[11] W. Blok and S. McGaugh *Ap. J.* **508**, 1 (1998).

[12] J. Bekenstein *Phys. Rev. D* **70**, 083509 (2004).

[13] A. De Felice and S. Tsujikawa, *Living Rev. Relativ.* **13**, 3 (2010).

[14] A. Starobinsky, *Phys. Lett.* B **91**, 1 (1980).

[15] L. Amendola and D. Tocchini-Valentini, *Phys. Rev.* D **64**, 043509 (2001); S. 'i. Nojiri and S. D. Odintsov, *PoS WC* **2004**, 024 (2004); G. Allemandi, A. Borowiec, M. Francaviglia and S. D. Odintsov, *Phys. Rev.* D **72**, 063505 (2005); T. Koivisto, *Class. Quantum Gravity* **23**, 4289 (2006).

[16] O. Bertolami, C. G. Boehmer, T. Harko and F. S. N. Lobo, *Phys. Rev.* D **75**, 104016 (2007).

[17] I. T. Drummond and S. J. Hathrell, *Phys. Rev.* D **22**, 343 (1980).

[18] H. F. M. Goenner, *Found. Phys.* **14**, 865 (1984).

[19] O. Bertolami, P. Frazão and J. Páramos, *Phys. Rev.* D **81**, 104046 (2010).

[20] O. Bertolami and J. Páramos, *Phys. Rev.* D **84**, 064022 (2011).

[21] S. Nojiri, S. D. Odintsov, *Phys. Rev.* D **72**, 063505 (2005).

[22] O. Bertolami and J. Páramos, *Phys. Rev.* D **84**, 064022 (2011).

[23] O. Bertolami and J. Páramos, *Gen. Relativity and Gravitation* **47**, 1835 (2014).

[24] J. Páramos and C. Bastos, *Phys. Rev.* D **86**, 103007 (2012).

[25] N. Castel-Branco , J. Páramos and R. March, *Phys. Lett.* B **735**, 25 (2014).

[26] O. Bertolami and J. Páramos, *Class. Quantum Gravity* **25**, 245017 (2008).

[27] O. Bertolami, P. Frazão and J. Páramos, *Phys. Rev.* D **86**, 044034 (2012).

[28] O. Bertolami and M. C. Sequeira, *Phys. Rev.* D **79**, 104010 (2009).

[29] O. Bertolami and J. Páramos, *Gen. Relativity and Gravitation* **48** no.3, 34 (2016).

[30] O. Bertolami and J. Páramos, *Int. J. Geom. Meth. Mod. Phys.* **11**, 1460003 (2014).

[31] O. Bertolami and J. Páramos, *JCAP* **2010**, 03 (2010).

[32] Mariusz Dabrowski *et al*, *Ann. Phys.* **18**, 1 (2009).

[33] C. Brans and R. Dicke *Phys. Rev. Lett.* **124**, 925 (1961).

[34] B. Whitt, *Phys. Lett.* **145**, 3 (1984).

[35] T. Damour and G. Esposito-Farese, *Class. Quantum Gravity* **9**, 2093 (1992).

[36] T. Sotiriou and V. Faraoni, *Class. Quantum Gravity* **25**, 20 (2008).

[37] O. Bertolami, F. S. N. Lobo and J. Páramos, *Phys. Rev.* D **78**, 064036 (2008).

[38] J. D. Brown, *Class. Quantum Gravity* **10**, 8 (1993).

[39] B. F. Schutz, *Phys. Rev. D* **2**, 2762 (1970).

[40] O. Bertolami and J. Páramos, *Class. Quantum Gravity* **25**, 124 (2008).

[41] O. Bertolami and J. Páramos, *Phys. Rev.* D **89**, 044012 (2014).

[42] R. Ribeiro and J. Páramos, *Phys. Rev.* D **90**, 124065 (2014).

[43] R. P. L. Azevedo and J. Páramos, *Phys. Rev.* D **94**, 064036 (2016).

[44] A. Einstein, Siz. Preuss. Acad. Scis. (1919); M. Henneaux, C. Teitelboim, *Phys. Lett.* B **222**, 195 (1989); W. G. Unruh, *Phys. Rev.* D **40**, 1048 (1989) ; W. G. Unruh and R. M. Wald, *Phys. Rev.* D **40**, 2598 (1989).

[45] J. F. Navarro, C. S. Frenk and S. D. M. White, *Ap. J.* **462**, 563 (1996).

[46] Y. Suto, S. Sasaki and N. Makino, *Ap. J.* **509**, 2 (1998).

[47] G. van de Ven, R. Mandelbaum and C. Keeton *Mon. Not. R. Astron. Soc.* **398**, 2 (2009).

[48] L. Hernquist, *Ap. J.* **356**, 359 (1990).

[49] A. Burkert *Ap. J. Lett.* **447**, 1 (1995).

[50] S. Hawking and G. Ellis, *Cambridge University Press*, (2010).

[51] O. Gerhard, A. Kronawitter, R. P. Saglia and R. Bender, *Ap. J.* **121**, 1936 (2001).

[52] A. Kronawitter, R. P. Saglia, O. Gerhard and R. Bender, *Astron. Astrophys. Suppl. Ser.* **144**, 53 (2000).